Nonlinear Excitation of Surface Plasmon Polaritons by Four-Wave Mixing

Stefano Palomba and Lukas Novotny*

Institute of Optics, University of Rochester, Rochester, New York, USA

(Received 4 April 2008; revised manuscript received 17 June 2008; published 1 August 2008)

We demonstrate nonlinear excitation of surface plasmons on a gold film by optical four-wave mixing. Two excitation beams of frequencies ω_1 and ω_2 are used in a modified Kretschmann configuration to induce a nonlinear polarization at a frequency of $\omega_{4\mathrm{wm}} = 2\omega_1 - \omega_2$, which gives rise to surface plasmon excitation at a frequency of $\omega_{4\mathrm{wm}}$. We observe a characteristic plasmon dip at the Kretschmann angle and explain its origin in terms of destructive interference. Despite a nonvanishing bulk response, surface plasmon excitation by four-wave mixing is dominated by a nonlinear *surface* polarization. To interpret and validate our results, we provide a comparison with second-harmonic generation.

DOI: 10.1103/PhysRevLett.101.056802 PACS numbers: 73.20.Mf, 42.65.Ky, 78.47.nj

The geometry-dependent excitations of a strongly coupled plasma (surface plasmons) give rise to unique optical properties, which are currently being explored for various photonic and electronic applications [1–3]. On planar or cylindrical metal interfaces, the momentum (wave vector) of surface plasmons is larger than the momentum associated with free propagating electromagnetic radiation [4,5] making it necessary to excite surface plasmons with evanescent waves [6–9]. The most widely employed surface plasmon excitation scheme is the Kretschmann configuration [8]. In this configuration, surface plasmon excitation is associated with characteristic dips in the angular reflectivity of a laser beam incident on a metal film deposited on the surface of a prism. Nonlinear studies of surface plasmon excitation on metal films have concentrated predominantly on second-order processes, such as second-harmonic generation (SHG) and sum-frequency generation [10–12]. The reason for using second-order processes lies in its simplicity and the ability to discriminate the bulk response from the surface response using the inversion symmetry of most metals [10,13]. For third-order processes, it can be expected that the bulk response strongly dominates over the surface response, and hence it is not *a priori* clear how effective third-order surface plasmon excitation is. In this Letter, we show that, despite the third-order bulk response, surface plasmons on metal films can be efficiently excited by four-wave mixing in the Kretschmann configuration. This result holds promise for applications in nonlinear plasmonics, e.g., surface plasmon amplification, surface plasmon switching, and manipulation.

We consider a gold film of thickness ~52 nm (roughness 1 nm rms, prepared by *e*-beam evaporation on glass) excited in a modified Kretschmann configuration (cf. Fig. 1) by two incident laser beams of frequencies ω_1 and ω_2, respectively. The metal's third-order susceptibility $\chi^{(3)}$ gives rise to a nonlinear polarization at frequency $\omega_{4\mathrm{wm}} = 2\omega_1 - \omega_2$, which leads to scattered radiation at the same frequency. The two laser beams are generated by a Ti:sapphire laser, providing pulses of duration ~200 fs and wavelength $\lambda_1 = 810$ nm, and an optical parametric oscillator, providing pulses of the same duration and wavelength $\lambda_2 = 1162$ nm. Both lasers have a repetition rate of 76 MHz, and the average powers are 3 and 12 mW, respectively. The spot diameters at the gold surface are 1.2 and 4 μm, respectively. The scattered light at the four-wave mixing frequency $\omega_{4\mathrm{wm}}$ has a wavelength of $\lambda_{4\mathrm{wm}} = 613$ nm.

As shown in Fig. 1, we use an oil-immersion objective of numerical aperture NA = 1.3 and magnification $M = 40$ to focus the incident laser beams on the metal surface and to collect the generated light at the four-wave mixing frequency. The different wavelengths are spectrally separated by optical filters (two bandpass filters 500 nm $< \lambda <$ 700 nm, two shortpass filters $\lambda < 750$ nm, a line filter $\lambda = 620 \pm 20$ nm, and a dichroic beam splitter reflecting $\lambda > 725$ nm). The angular resolution of the experiments is

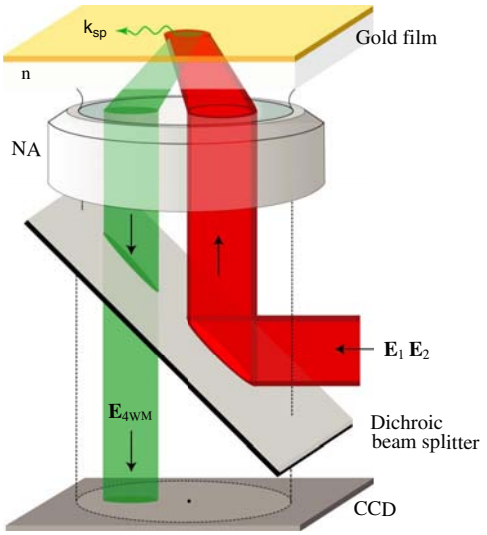

FIG. 1 (color online). Nonlinear excitation of surface plasmons. Two incident beams at frequencies ω_1 and ω_2 give rise to four-wave mixing at a gold film and generate an outgoing beam at frequency $\omega_{4\mathrm{wm}} = 2\omega_1$-$\omega_2$, which is projected onto a CCD. The lateral CCD coordinates correspond to the transverse wave vector k_x.

defined by the diameter of the incident laser beams relative to the size of the back aperture (13 mm) of the objective lens. The angle of emission is measured by projecting the scattered beam at $\omega_{4\mathrm{wm}}$ on a thermoelectrically cooled CCD. Thus, the displacement Δx of the detected spot on the CCD measured from the optical axis is a direct measure for the transverse wave vector $k_x = (k/f)\Delta x$ [14], with f being the focal length of the objective and $k = n\omega_{4\mathrm{wm}}/c$ being the wave vector of the emitted radiation.

The third-order susceptibility $\chi^{(3)}$ giving rise to four-wave mixing is a tensor of rank 3. Although the symmetry of our experimental configuration allows many components of the tensor to be eliminated, the number of unknowns remains high. Furthermore, in addition to the bulk response, we have to take into consideration the surface-specific response. Therefore, to establish an understanding for the observed third-order response, we relate our observations to SHG, which is a reasonably well understood second-order process [10–12]. In fact, for SHG the bulk response can be greatly ignored, and only two tensor components of the surface susceptibility $\chi_S^{(2)}$ need to be considered [10].

Thus, let us first consider SHG by two collinear excitation beams incident at the angle θ as shown in Fig. 2(a). The two beams are p-polarized and are incident from glass

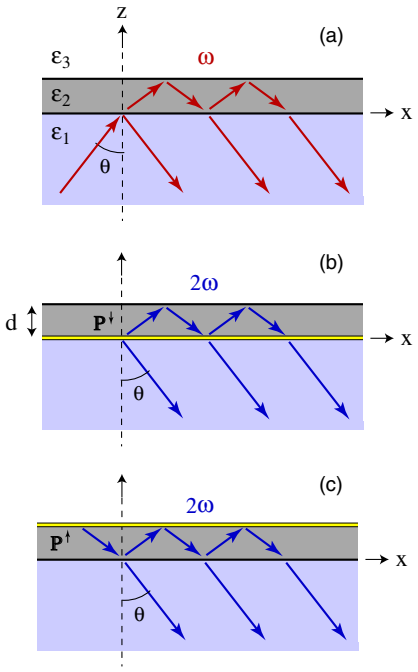

FIG. 2 (color online). Illustration of nonlinear surface plasmon excitation by SHG. (a) The incident laser field generates nonlinear surface polarizations at the lower and upper gold interfaces. (b) The nonlinear polarization $\mathbf{P}^{\downarrow}$ at the lower interface acts as a source for a secondary field at the nonlinear frequency 2ω. (c) The same holds for the polarization $\mathbf{P}^{\uparrow}$ at the upper interface.

($\varepsilon_1 = 2.25$) onto a gold film of thickness d and dielectric function $\varepsilon_2(\omega)$. It has been demonstrated that the largest contribution to the nonlinear signal at frequency 2ω originates from a second-order surface susceptibility $\chi^{(2)}_{S,xzx}$ [10,15], where the indices indicate field components parallel (x) and perpendicular (z) to the interface, respectively. The incident waves are represented as

$$\mathbf{E}(\omega) = E_0[(k_{1z}/k_1)\mathbf{n}_x - (k_x/k_1)\mathbf{n}_z]e^{ik_x x + ik_{1z} z - i\omega t}, \quad (1)$$

where $\mathbf{k}_1 = [k_x, 0, k_{1z}]$ and $k_1^2 = \varepsilon_1(\omega/c)^2$. $\mathbf{n}_x$ and $\mathbf{n}_z$ are unit vectors in the x and z directions, respectively. The components of the $\mathbf{k}_1$ vector are determined by the angle of incidence θ according to $k_x = k_1 \cos\theta$ and $k_{1z} = k_1 \sin\theta$. As illustrated in Figs. 2(b) and 2(c), we consider two interfaces. The surface polarization at the second-harmonic frequency on the bottom interface is calculated as

$$\begin{aligned} P_x^{\downarrow}(2\omega) &= \varepsilon_o \chi^{(2)}_{S,xzx}(2\omega;\omega,\omega) E_z(\omega) E_x(\omega) \\ &= \varepsilon_o \chi^{(2)}_{S,xzx} E_0^2 \frac{\varepsilon_1}{\varepsilon_2}\left[1 + \frac{r_{12} + r_{23}\exp(2ik_{2z}d)}{1 + r_{12}r_{23}\exp(2ik_{2z}d)}\right] \\ &\quad \times \left[1 - \frac{r_{12} + r_{23}\exp(2ik_{2z}d)}{1 + r_{12}r_{23}\exp(2ik_{2z}d)}\right] \\ &\quad \times \frac{k_x k_{1z}}{k_1^2} e^{2ik_x x - 2i\omega t}, \end{aligned} \quad (2)$$

where we have used the single-interface Fresnel reflection and transmission coefficients for p polarization [16]. Notice that both exciting fields (E_z and E_x) are evaluated on the gold side of the interface and that all quantities are evaluated at the frequency ω. Also, $k_{2z} = \sqrt{k_2^2 - k_x^2}$.

The polarization $P_x^{\downarrow}$ now acts as a source current at the second-harmonic frequency, and the resulting field $\mathbf{E}(2\omega)$ is calculated as

$$\mathbf{E}(\mathbf{r}, 2\omega) = \frac{(2\omega/c)^2}{\varepsilon_o} \int_{\mathrm{surface}} \overleftrightarrow{\mathbf{G}}(\mathbf{r}, \mathbf{r}'; 2\omega)\mathbf{P}^{\downarrow}(\mathbf{r}', 2\omega) d\mathbf{r}'. \quad (3)$$

The field radiated into the upper space is reflected from the top boundary and then superimposed to the field emitted into the lower space. The total field in the lower half-space due to the polarization $P_x^{\downarrow}$ is then calculated to be [17]

$$\begin{aligned} \mathbf{E}^{\downarrow}(2\omega) &= \frac{P_x^{\downarrow}}{2\varepsilon_o}\left[\frac{k_1}{\varepsilon_1} + \frac{k_2}{\varepsilon_2}\frac{r_{23}t_{21}\exp(2ik_{2z}d)}{1 + r_{12}r_{23}\exp(2ik_{2z}d)}\right] \\ &\quad \times [(k_{1z}/k_1)\mathbf{n}_x + 2(k_x/k_1)\mathbf{n}_z]e^{-ik_{1z}z}, \end{aligned} \quad (4)$$

where all quantities are evaluated at the second-harmonic frequency 2ω. The coupling to the surface plasmons propagating at the top interface is dominated by the poles of the r_{23} term, i.e., $k_{2z}\varepsilon_3 + k_{3z}\varepsilon_2 = 0$. Efficient coupling to surface plasmons results in strong leakage radiation [18]. However, the latter interferes with the nonlinear field emitted from the lower interface. This interference is repre-

sented by the two terms in the brackets in Eq. (4) and gives rise to the observed "plasmon dip" as discussed later.

We now turn to the fields generated by the polarization $P_x^{\uparrow}$ at the upper interface, as illustrated in Fig. 2(c). We find

$$P_x^{\uparrow}(2\omega) = \varepsilon_o \chi_{xzx}^{(2)} E_0^2 \left[\frac{t_{12}(1 + r_{23})\exp(ik_{2z}d)}{1 + r_{12}r_{23}\exp(2ik_{2z}d)}\right] \times \left[\frac{t_{12}(1 - r_{23})\exp(ik_{2z}d)}{1 + r_{12}r_{23}\exp(2ik_{2z}d)}\right] \frac{k_x k_{2z}}{k_2^2} e^{2ik_x x - 2i\omega t}. \quad (5)$$

As in Eq. (2), all quantities are to be evaluated at the fundamental frequency ω. Using $P_x^{\uparrow}$ as the source current in Eq. (3), we find for the nonlinear field emitted into the lower half-space

$$\mathbf{E}^{\uparrow}(2\omega) = \frac{P_x^{\uparrow}}{2\varepsilon_o}\frac{k_2}{\varepsilon_2}\left[\frac{t_{21}\exp(ik_{2z}d)}{1 + r_{12}r_{23}\exp(2ik_{2z}d)}\right] \times [(k_{1z}/k_1)\mathbf{n}_x + 2(k_x/k_1)\mathbf{n}_z]e^{-ik_{1z}z}, \quad (6)$$

where all quantities are to be evaluated at the nonlinear frequency 2ω. $\mathbf{E}^{\uparrow}$ has only a single term, and hence plasmon excitation is observed through leakage radiation, i.e., a peak at the Kretschmann angle (calculated for 2ω). The total detected intensity in the lower half-space is calculated as $I(\theta, 2\omega) \propto |\mathbf{E}^{\downarrow} + \mathbf{E}^{\uparrow}|^2$ and is shown in Fig. 3(a) for an excitation wavelength of $\lambda = 2\pi c/\omega = 1162$ nm. The two main features in the theoretical curve are a peak at $\theta \approx 42°$ and a dip at $\theta \approx 46°$. The dip originates from the interference of SH light emitted from the bottom interface [cf. Fig. 2(b)], as described by Eq. (4). The dip is associated with surface plasmon excitation at a wavelength of $\lambda = 581$ nm. On the other hand, the narrow peak is due to surface plasmon excitation at a wavelength of $\lambda = 1156$ nm and originates from the r_{23} term in Eq. (6). This peak has been documented before for the case of a silver film [11].

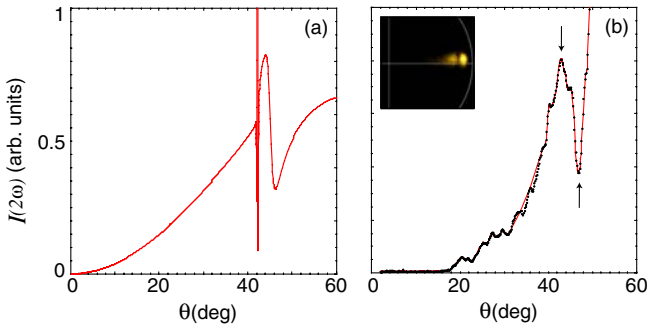

FIG. 3 (color online). Second-harmonic generation from a 52 nm gold film on a glass substrate excited at a wavelength of $\lambda = 1162$ nm. (a) Theoretical curve revealing a plasmon peak and a plasmon dip. (b) Experimental curve acquired with the setup shown in Fig. 1. The inset shows an image of the recorded SH light showing the plasmon dip at $\theta \approx 46°$.

Figure 3(b) shows our experimental results for the angular dependence of SHG. Besides some bumps due to laser beam inhomogeneities and surface roughness, the experimental curve is in good agreement with the predicted theoretical behavior in Fig. 3(a). Because of the finite pixel size of our CCD camera, the experimental angular resolution is limited to $\approx 0.4°$ and does not allow us to resolve the narrow plasmon peak at $\theta \approx 42°$. Instead, the plasmon peak appears as a smoothed-out bump indicated by the arrow. On the other hand, the plasmon dip at $\theta \approx 46°$ is clearly resolved and can be identified as originating from the destructive interference of leakage radiation from the SH surface plasmon and SH radiation emitted from the bottom interface. The inset in Fig. 3(b) shows a CCD image for the case where the SH beam overlaps with the Kretschmann angle. For angles θ beyond the Kretschmann angle, the experimental curve starts to deviate from the theoretical one, which is most likely due to $\chi_{zzz}^{(2)}$, a contribution that has not been taken into account in our theory and that increases in strength for large θ.

Having identified the main mechanisms of surface plasmon excitation by second-harmonic generation, we now discuss our experimental results based on four-wave mixing (4WM). The nonlinear polarization is determined by the input beams as

$$\mathbf{P}(\omega_{4\mathrm{wm}} = 2\omega_1 - \omega_2) = \varepsilon_o \chi^{(3)} \mathbf{E}(\omega_1)\mathbf{E}(\omega_1)\mathbf{E}^*(\omega_2). \quad (7)$$

We have three different contributions: the two interfaces and the bulk. As outlined before, $\chi^{(3)}$ is a tensor of rank 3, and the theoretical analysis will strongly depend on the tensor elements that are admitted in the model. We avoid laying out the entire theory as the basic elements are well conveyed by the second-harmonic analysis described above. Our goal is to demonstrate that, despite the bulk contribution of $\chi^{(3)}$, surface plasmons at the frequency $\omega_{4\mathrm{wm}}$ are efficiently excited by a nonlinear surface polarization at the glass-metal interface. Similar to second-harmonic generation, we expect to observe a characteristic four-wave mixing dip at the Kretschmann angle generated by destructive interference of plasmon leakage radiation from the top interface and direct radiation from the bottom interface.

As shown in Fig. 4, we clearly observe the predicted plasmon dip in the emission patterns. In Figs. 4(a) and 4(b), we expanded the incident excitation beams in order to cover a broad range of angles θ. Both incident beams are p-polarized in Fig. 4(a) and s-polarized in Fig. 4(b). Evidently, the dip is observed only for p-polarized excitation, which proves that a surface plasmon is excited at the four-wave mixing wavelength $\lambda_{4\mathrm{wm}} = 613$ nm. For s-polarized excitation, the 4WM signal is still measurable, but the dip is not present anymore. The 4WM signal exists even if the excitation beams are centered on the optical axis [moved towards the cross-hair in Figs. 4(a) and 4(b)],

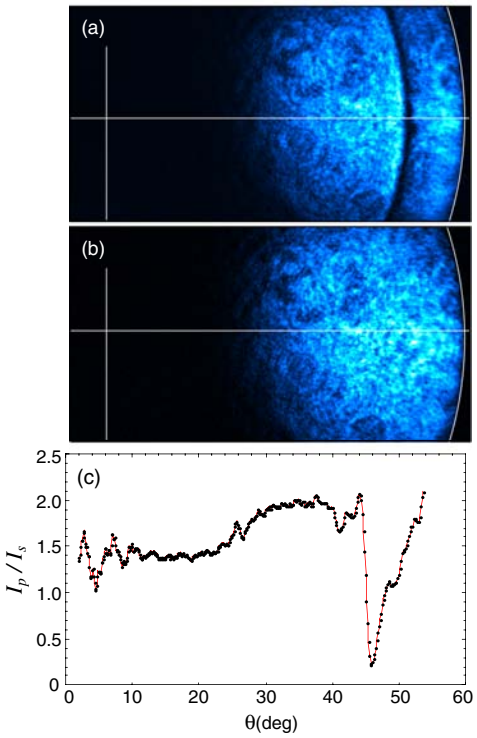

FIG. 4 (color online). Nonlinear four-wave mixing at a 52 nm gold film on a glass substrate. (a),(b) CCD images using expanded excitation beams. (a) p-polarized excitation beams; (b) s-polarized excitation beams. (c) Angular dependence of four-wave mixing radiation ($\lambda_{4\mathrm{wm}} = 613$ nm). The curve shows the ratio of four-wave mixing intensity generated by p-polarized excitation (I_p) and four-wave mixing intensity generated by s-polarized excitation (I_s).

which suggests that both bulk *and* surface nonlinearities are involved in the four-wave mixing mechanism. Figure 4(c) plots the normalized 4WM signal over the entire range of incident angles θ. The graph represents the ratio of four-wave mixing intensity generated by p-polarized excitation (I_p) and four-wave mixing intensity generated by s-polarized excitation (I_s). The normalization is performed in order to remove any possible artifacts due to diffraction at the rims of the backaperture and due to spectral and angular variations of the objective's transmissivity. Interestingly, the emitted 4WM radiation is predominantly p-polarized even if the incident waves are s-polarized. Additionally, for p-polarized excitation, the total emitted intensity at $\omega_{4\mathrm{wm}}$ is approximately twice as strong as the intensity generated by s-polarized excitation. These observations indicate that the third-order *surface* polarization is a dominant contribution in nonlinear four-wave mixing at metal films.

In conclusion, we used nonlinear four-wave mixing to excite surface plasmons on a gold film. A characteristic plasmon dip at the Kretschmann angle indicates that the dominating nonlinear contribution is a third-order *surface* susceptibility. As in the case of SHG [cf. Fig. 2(a)], this dip originates from a nonlinear surface polarization $P_x^{\downarrow}(\omega_{4\mathrm{wm}})$ at the lower gold interface. $P_x^{\downarrow}$ gives rise to radiation at frequency $\omega_{4\mathrm{wm}}$ emitted into both the lower half-space (glass substrate) and the metal film. The latter excites surface plasmons at the upper gold interface, and the resulting leakage radiation interferes destructively with the radiation emitted directly into the lower half-space. This interference is phase-sensitive, and the appearance of a dip requires a clear phase separation between the two interfering components. No dip would be expected if the third-order nonlinearity were entirely associated with a bulk response. We hence conclude that surface plasmon excitation by four-wave mixing is dominated by a third-order *surface* nonlinearity.

We thank Giovanni Piredda for stimulating discussions. This work was supported by the U.S. Department of Energy under Grant No. DE-FG02-01ER15204.

*http://www.nano-optics.org

[1] *Surface Plasmon Nanophotonics*, edited by M. L. Brongersma and P. G. Kik (Springer, Dordrecht, 2007).
[2] S. A. Maier, *Plasmonics: Fundamentals and Applications* (Springer, New York, 2007).
[3] E. Ozbay, Science **311**, 189 (2006).
[4] A. Sommerfield, Ann. Phys. Chemie **67**, 233 (1899).
[5] J. Zenneck, Ann. Phys. **23**, 846 (1907).
[6] E. Devaux, T. W. Ebbesen, J. C. Weeber, and A. Dereux, Appl. Phys. Lett. **83**, 4936 (2003).
[7] B. Hecht *et al.* Phys. Rev. Lett. **77**, 1889 (1996).
[8] E. Kretschmann and H. Raether, Z. Naturforsch. A **23**, 2135 (1968).
[9] A. Otto, Z. Phys. **216**, 398 (1968).
[10] Y. R. Shen, *The Principles of Nonlinear Optics* (Wiley, New York, 1984).
[11] H. J. Simon, D. E. Mitchell, and J. G. Watson, Phys. Rev. Lett. **33**, 1531 (1974).
[12] H. J. Simon, R. E. Benner, and J. G. Rako, Opt. Commun. **23**, 245 (1977).
[13] Y. R. Shen, Nature (London) **337**, 519 (1989).
[14] A. Bouhelier *et al.*, Opt. Lett. **32**, 2535 (2007).
[15] P. Guyot-Sionnest and Y. R. Shen, Phys. Rev. B **38**, 7985 (1988).
[16] M. Born and E. Wolf, *Principles of Optics* (Cambridge University Press, Cambridge, 1980).
[17] The fields can be derived using the Green's function in the form $[\overleftrightarrow{\mathbf{I}} + k(\mathbf{r})^{-2}\nabla\nabla]G_o(\mathbf{r}, \mathbf{r}')$ and expressing the scalar Green's function G_o in terms of the Weyl identity.
[18] A. Bouhelier and G. P. Wiederrecht, Opt. Lett. **30**, 884 (2005).